INELASTIC πN COLLISIONS

D.I. Blokhintsev, V.S. Barashenkov, Wang Yung,
E.K. Mihul, Huang Tzu-tzan and Hu-Schi-kei.
Joint Institute of Nuclear Research, Dubna.

I. PERIPHERAL AND CENTRAL COLLISIONS

In the present state of the theory, the quantitative characteristics of the strong interaction processes can be obtained only on the basis of quite definite assumptions on the mechanism of the phenomenon. These assumptions may be given in the form of a simple physical picture or in a more abstract form of some assumptions concerning the behaviour of an amplitude in the complex plane.

For a long time the Fermi - Landau theory served as such a model theory. At the CERN Symposium in 1956, one of the authors criticized this theory and suggested separating the inelastic interactions into "central" and "peripheral"[1,2]. Now a lot of new information on the NN and πN collisions has been obtained, and many calculations have been made[3-7].

It now seems that this more detailed picture of the strong collisions is in reasonable agreement with new experimental data, which however are not very precise.

In the following, the calculations of πN interaction are described which were recently performed at Dubna based on the physical picture of two types of collision.

II. SCHEME OF CALCULATIONS

The calculation is based on the one-pion mechanism of the momentum transfer from a pion to a nucleon.

In Fig. 1 typical diagrams are drawn. As is seen, one should distinguish between the processes with even and odd numbers of pions. In

the first case the main process is the pion production in the peripheral collision (diagram A). In the case of odd number of pions this process is accompanied by the production of a pion during the scattering of a virtual pion on a nucleon (diagram B).

The process represented in Fig. 1 by the diagram A′ can compete with that shown by diagram A. Just in the same manner, the process B may be imitated by the process given by diagram B′.

It has been shown by Rodberg[8] that the diagram (a) corresponding to the interaction with the nucleon core (see Fig. 2) makes a considerably smaller contribution than the diagram (b) (see Fig. 2b) representing the $\pi\pi$ interaction. These diagrams enter as components into the diagrams drawn in Fig. 1. For this reason we neglect the contribution of the diagram A′ compared with the contribution of the diagram A. The same consideration holds for diagrams B and B′.

Therefore, it is sufficient to consider the processes A and B. The corresponding cross-sections have the form:

$$\sigma_{2n}(E) = g^2 \frac{2\pi^2}{v} \int_0^{q_{max}} \frac{q^2 dq}{4 q_0 p_0 \omega} \sigma_{\pi\pi}^{(2n)}(Q) 2 \sqrt{1 - \left(\frac{2\mu}{Q}\right)^2} \frac{Q^2}{(2\pi)^4} \times$$

$$\times \left\{ \frac{1}{4pq} \ln \left(1 + \frac{4pq}{2p_0 q_0 - 2pq - 2M^2 + \mu^2} \right) - \right.$$

$$\left. - \frac{\mu^2}{(2p_0 q_0 - 2M^2 + \mu^2)^2 - 4p^2 q^2} \right\} \qquad (1)$$

$$\sigma_{2n+1}(E) = \frac{2\pi}{v} \int_0^{P_{max}} \frac{P^2 dP}{p_0 \omega} \int_{\sqrt{p^2 + (M+\mu)^2}}^{E - \sqrt{p^2 + m^2}} 2 \cdot \frac{S^2}{(2\pi)^4} \sqrt{1 - \left(\frac{2\mu}{S}\right)^2} \cdot \sigma_{\pi\pi}^{(2n)}(S) dP_0 \times$$

$$\times \frac{2\sigma_{\pi N}(R) \sqrt{\frac{1}{4}(R^2 - M^2 - \mu^2)^2 - M^2\mu^2}}{(2P_0 p_0 - M^2 - R^2 + \mu^2)^2 - 4P^2 p^2} . \qquad (2)$$

Here $q_{max} = \frac{1}{2E}\sqrt{(E+M+m)(E+M-m)(E-M+m)(E-M-m)}$;

$S^2 = (E-P_0)-P^2$; $Q^2 = (E-q_0)^2-q^2$; $R^2 = P_0^2-P^2$, $P_{max} = q_{max}/_{m\to m+\mu}$;

E is the total energy of primary particles in the c.m. system;

$p_0^2 = p^2 + M^2$;

$q_0^2 = q^2 + M^2$;

p is the momentum of a primary nucleon in the c.m. system;

M is its mass;

m is the sum of the mass of particles produced in $\pi\pi$ collision;

v is the relative velocity of π and N in the c.m. system;

$\sigma_{\pi\pi}^{(2n)}$ is the cross-section for $\pi\pi$ interaction;

g^2 is the coupling constant πN ;

ω and μ are the energy and mass of π in the c.m. system.

The calculation shows that the diagrams of the type B give a much smaller contribution to πN interaction than the diagrams of the type A. The following table gives the ratios of the cross-sections for the even and odd number of pions at different energies.

Table I

The energy of a primary pion in the lab. system (GeV)	$\frac{\sigma_3}{\sigma_2}$	$\frac{\sigma_5}{\sigma_4}$
2	0.1	-
7	0.15	-
100	1	0.25
1000	2	0.5

The data given in this table show that the study of the events with odd number of pions at a high energy of a primary pion is a tool to study the nucleon core. However, it should be borne in mind that these channels are of minor importance. The production of a greater even number of pions will be the predominant process at these high energies.

To calculate the relative multiplicity of pions, momentum transfer, and the angular distributions, we need to know the partial cross-sections for $\pi\pi$ interaction. These partial cross-sections have been calculated by assuming the absence of correlations between the particles produced in $\pi\pi$ collision. Such an assumption leads to the factorization of the matrix element of particle production in $\pi\pi$ collisions: $\sim \Omega^{n-1}(E)\rho_n(E)$, where E is the energy of primary particles in the c.m. system; $\rho_n(E)$ is the phase space for n particles, and $\Omega(E)$ is a certain three-dimensional volume. The calculations have been made under the assumption corresponding to the Fermi theory

$$\Omega(E) = \frac{4\pi}{3}\left(\frac{\hbar}{\mu c}\right)^3 \frac{Mc^2}{E} \quad *) .$$

By assuming the inelastic cross-section for πN collision to be 23 mb, and the constant for πN interaction to be $g^2 = 14.5$, it is possible to get from Eqs. (1) and (2) the effective cross-section for $\pi\pi$ interaction; it turns out to be $\sim$ 30 mb.

It should be emphasized that in calculating the statistical weight $S_n(E)$ the $\pi\pi$ resonance for $M^*_{\pi\pi} = 0.6$ M was taken into account, and the channels up to n = 8 were taken into consideration.

III. RESULTS OF CALCULATIONS

In Fig. 3 are given the results of calculations on the multiplicity of the pions for the total number of pions $\bar{n}$, and for the charged pions $\bar{n}^{\pm}$. The curve shows the increase of $\bar{n}$ with energy, in good agreement with the experimental data [see Refs. 3-5)].

In Fig. 4 the spectrum of the recoil protons (c.m.s.) is drawn for the pion energy $E_0 = 7$ GeV (lab. system). As we see, this spectrum fits to Duba data quite well[4]. **)

---

*) The additional assumption on the absence of the correlations between the initial and final states leads to $\Omega(E) = \text{const.}$ (Sudarshan's theory). Practically, both assumptions give close results.

**) The calculations have been made in more detail for $E_0 = 7$ GeV.

Fig. 5 shows the angular distribution of the recoil protons for the same pion energy. As is seen, the agreement for E_0 = 7 GeV is quite satisfactory.

In Table II are listed the mean values of the momentum of the recoil nucleon $\bar{p}$ and the mean values of its transverse momentum $\bar{p}_\perp$.

Table II

The kinetic energy of a primary pion E_0 GeV (lab.system)	The mean momentum of the recoil nucleon $\bar{p}$ GeV/c		The mean transverse momentum of the recoil nucleon $\bar{p}_\perp$ GeV/c	
	Theory	Experiment	Theory	Experiment
3	0.5	-	0.3	-
7	0.8	0.89 ± 0.04	0.4	0.37 ± 0.04
10	0.8	-	0.45	-
16	1.15	-	0.45	0.4

As is seen from this table, the theoretical values of $\bar{p}$ and $\bar{p}_\perp$ are not far from the experimental values and change very slowly. It is important that $\bar{p}_\perp$ is not great.

One can draw a conclusion from the calculations made, that the one-pion mechanism and the $\pi\pi$ interaction are important and predominant in the πN interaction. The central collisions do not seem to be so significant. Therefore to study the core of a nucleon, physics of "15% accuracy", experimental as well as theoretical, is not enough.

* * *

REFERENCES

1) D.I. Blokhintsev, Proc. of the CERN Symposium on High-Energy Accelerators, Vol. 2, 155 (1956).

2) D.I. Blokhintsev, V.S. Barashenkov and B.M. Barbashev, Uspekhi fiz. nauk. 68, 417 (1959).

3) V.S. Barashenkov, Nuovo Cimento 14, 656 (1959).

4) V.A. Belyakov, Wang Shu-fen, V.V. Glagolev et al. Preprint of JINR, P-530.

5) Proceedings of the 1960 Ann. Int. Conf. on High-Energy Physics (Rochester).

6) R. Hagedorn, Fort. d. Phys. 9, 1 (1961).

7) V.S. Barashenkov, Fort. d. Phys. 9, 42 (1961).

8) L. Rodberg, Phys.Rev.Letters 3, 58 (1959).

* * *

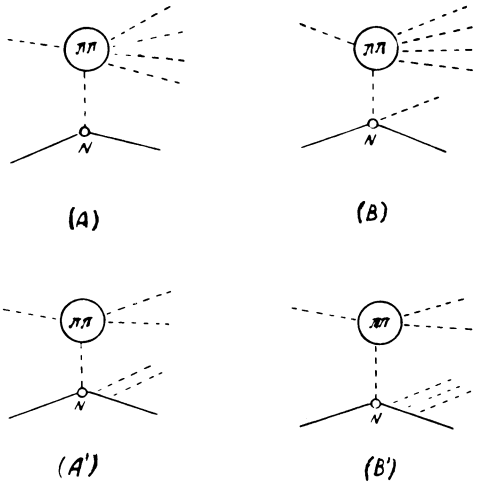

Fig. 1. The most important typical diagrams (A and B) for inelastic πN scattering, and the diagrams (A' and B') -- less essential.

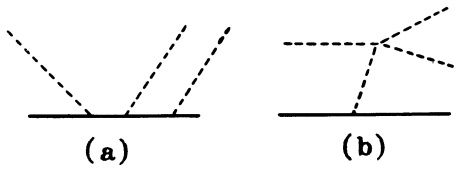

Fig. 2. The diagram (a) has a much smaller amplitude than the diagram (b).

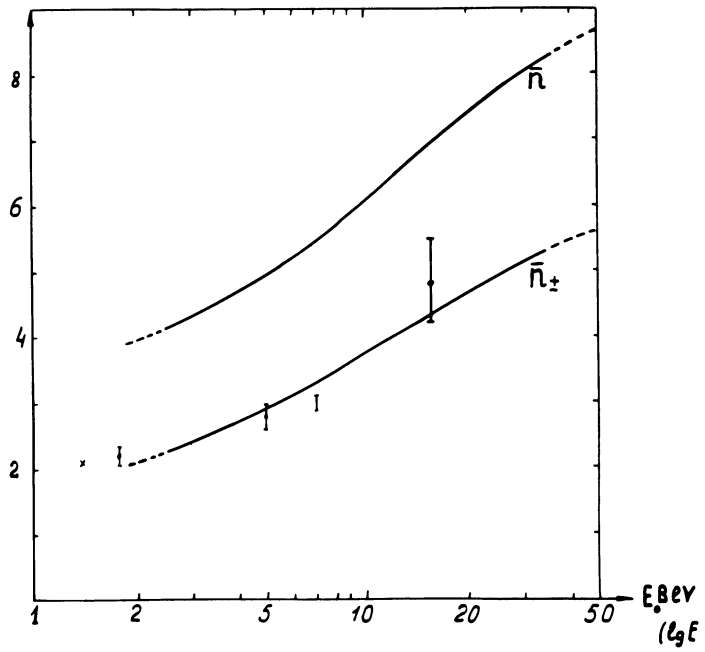

Fig. 3. The average number of particles produced in πp collisions at different energies of a primary pion (lab. system). $\bar{n}$ is the total number, $\bar{n}^{\pm}$ is the number of charged particles. These values incorporate also the recoil nucleon.

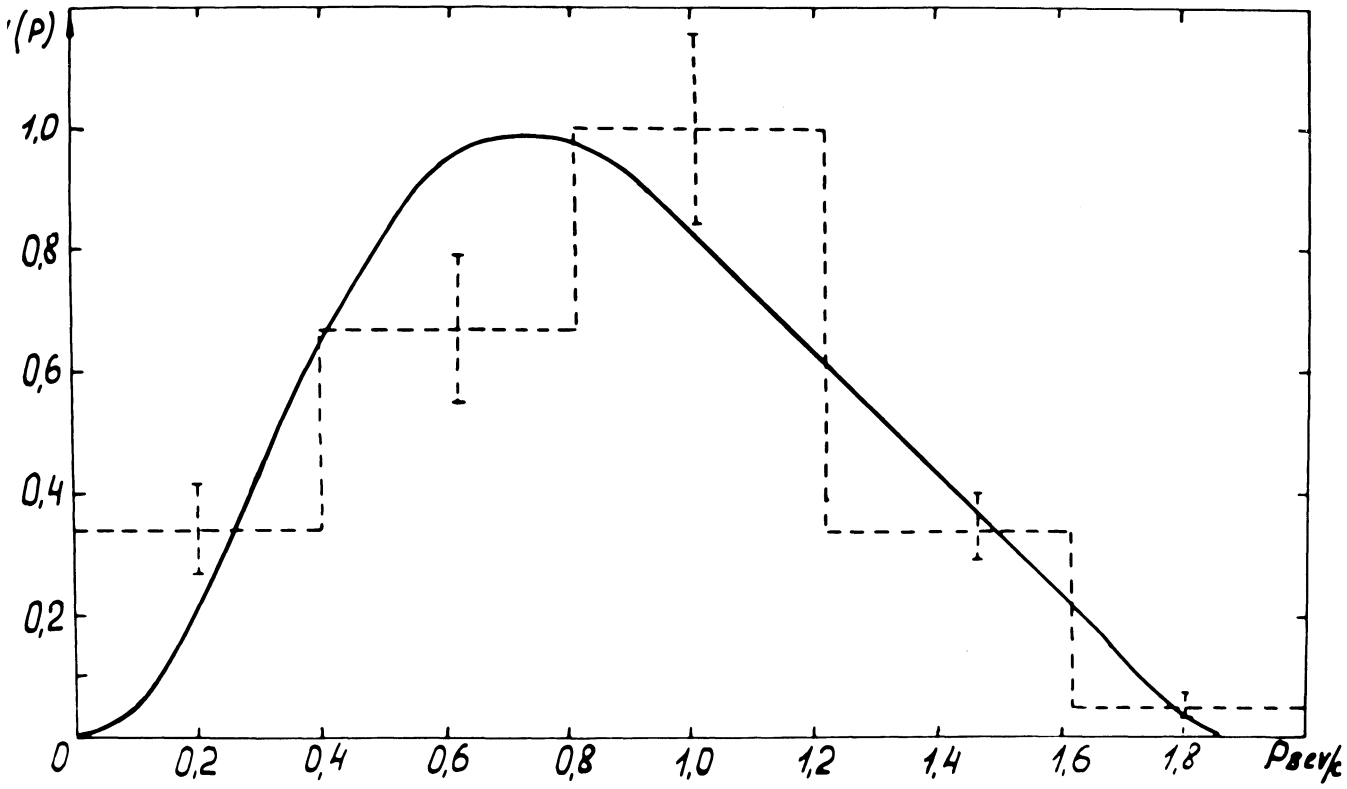

Fig. 4. The momentum spectrum of the recoil protons (c.m.s.) at an energy of the incident pion E_0 = 7 GeV. The dotted line indicates the experimental histogram from Ref. 4).

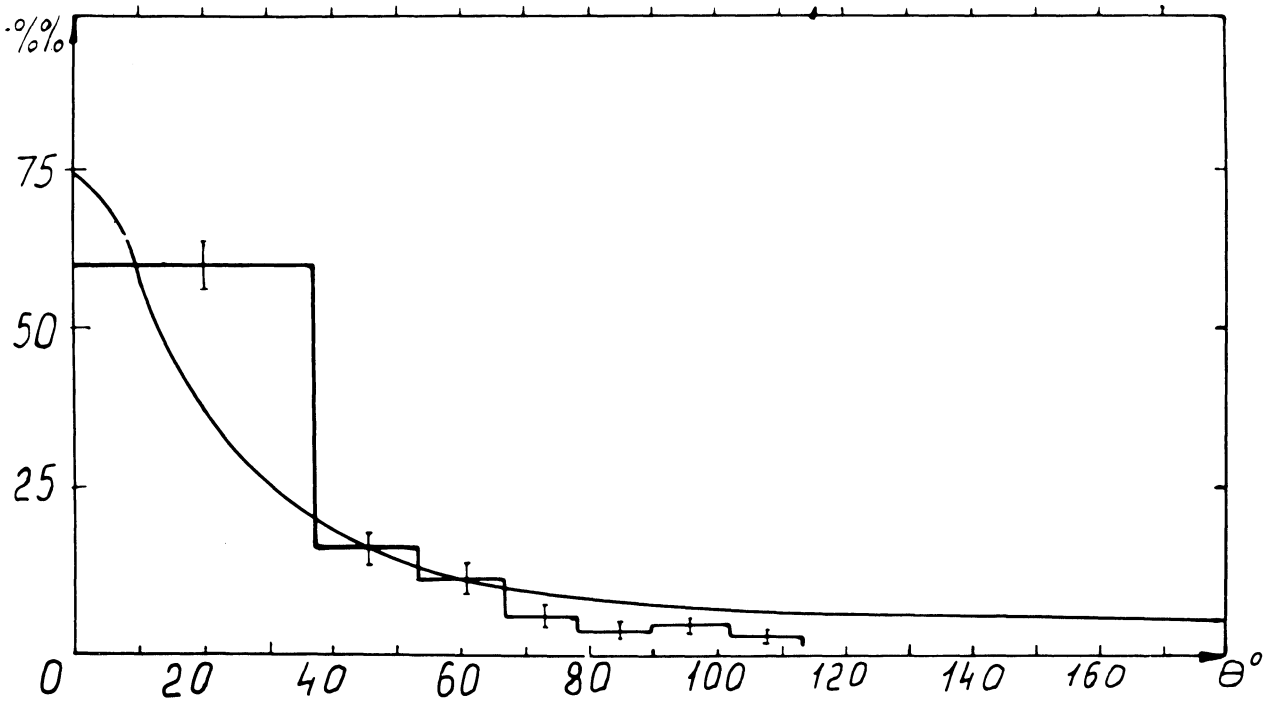

Fig. 5. The angular distribution of the recoil protons (c.m.s.) at an energy of the incident pion E_0 = 7 GeV. The dotted line indicates the experimental histogram from Ref. 4).